Analytical Methods

Accepted Manuscript

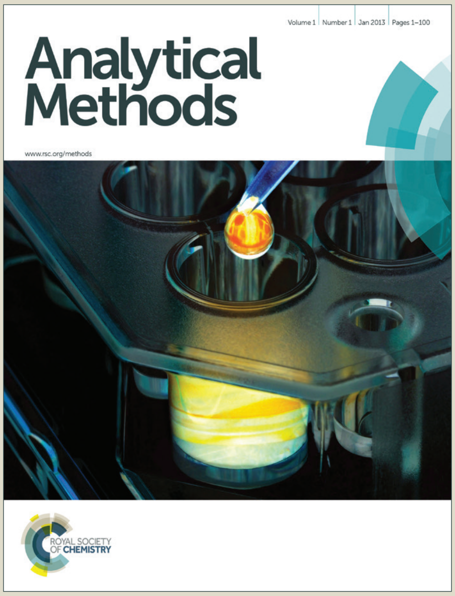

ROYAL SOCIETY OF CHEMISTRY

www.rsc.org/methods

A voltammetric Sensor based on Multi-Walled Carbon Nanotubes-MnO_2 nanowires composite film for simultaneous determination of hydroquinone and catechol

Jing Tang,[a b] *Baokang Jin,*[a]*

[a] Department of Chemistry and Engineering, Anhui University, 230601, Hefei, China
[b] College of Chemistry and Material Engineering, Anhui Science and Technology University, 244100, Fengyang, China
* e-mail: bkjinhf@aliyun.com

Abstract

A simple and sensitive electrochemical method for the simultaneous detection of hydroquinone (HQ) and catechol (CC) was developed, based on a multi-walled carbon nanotubes and MnO_2 nanowires composite (MWCNTs-MnO_2) modified glassy carbon electrode (GCE). Electrochemical impedance spectra studies showed a small charge transfer resistance (R_{ct}) of the MWCNTs-MnO_2 composite film due to the incorporation of MWCNTs. Compared with the bare GCE, both HQ and CC exhibited well-defined redox peaks and much larger peak currents at MWCNTs-MnO_2/GCE, which was related to the higher specific surface area and catalysis of MWCNTs-MnO_2 film. MnO_2 film acted as an electron transfer mediator to accelerate electron transfer rate for oxidation of HQ and CC. Due to the large separation of oxidation peak potentials (102 mV), the concentrations of HQ and CC can be easily determined simultaneously. The oxidation peak currents were linear to HQ/CC in the range from 5×10^{-7} to 8×10^{-5} M with the detection limits of 5×10^{-8} M (S/N=3) for HQ and 8×10^{-8} M (S/N=3) for CC, respectively. Simultaneous determination of HQ and CC with such electrode was conducted in tap water samples with reliable recovery.

Keywords: Multi-walled carbon nanotubes; MnO_2; Hydroquinone; Catechol; Simultaneous determination

1.Introduction

Hydroquinone (1, 4-dihydroxybenzene, HQ) and catechol (1, 2-dihydroxybenzene, CC) are two important isomers of phenolic compounds being widely used in dyes, paints, cosmetics and photographic chemicals [1, 2]. Otherwise, toxicity for aquatic life was an internal property in so many reports [3]. Because of similar structures and properties for HQ and CC, it is a challenge to directly and simultaneously determine two isomers. Therefore, the design and development of effective analytical methods for the simultaneous determination of the isomers are thus necessary. Up to date, several conventional techniques have been developed in the determination of two isomers analysis, such as high performance liquid chromatography [4,5], chemiluminescence [6], spectrophotometry [7], electrochemical methods [8] and so on, and electrochemical methods are preferable and attractive because of their fast operation, low maintenance costs, time saving and high sensitivity for the determination of dihydroxybenzene isomers.

Direct determination of dihydroxybenzene isomers at unmodified electrodes such as glass carbon and gold electrodes is a challenge due to board and overlap of their oxidation-reduction peaks. Thus, new materials have been developed to modified electrode to achieve simultaneous determination of HQ and CC, such as carbon nanotubes [9], graphene [10], mesoporous Pt [11] and ordered mesoporous carbon [12]. Among them, carbon nanotubes have the ability to promote electron-transfer reactions used as an electrode modified material in many electrochemical reactions [13], and moreover, it can be combined with other materials, such as metal [14, 15], metal oxide [16, 17] and metal hydroxide [18], which enhance their functionalities and exhibit synergistic effects with different applications in various fields. Recently, MnO_2-based materials modified electrodes have been used in many aspects, for electro-oxidation of H_2O_2 [19, 20], glucose [21] and aliphatic polyols [22], *etc*, especially MnO_2 film with good electrocatalytic properties [23], such as application as non-enzymatic hydrogen peroxide sensor reported by Luo et al.[24]. MnO_2 has a poor electrical conductivity for determination of HQ and CC, and improvements are needed. CNTs with high specific surface area and unique electronic properties, can be used as a good support for MnO_2 nanoparticles to realize optimized utilization of active sites. Therefore, MnO_2/CNTs nanocomposite has been used for fabricating electrochemical sensors for detecting glucose [25] or hydrazine [17]. However, to our knowledge, there are no reports on employing MWCNTs and MnO_2 nanocomposite as an electrode sensing material towards HQ and CC.

In the present work, a MWCNTs–MnO_2 hybrid material by a simple grinding method was prepared for simultaneous determination of HQ and CC. It was found that the MWCNTs–MnO_2 modified electrode exhibited high electrocatalytic activity towards HQ and CC with the separated anodic peak potential of 102 mV. Furthermore, due to its high electroactivity, selectivity and stability, satisfactory determination effect can be obtained with our MWCNTs–MnO_2/GCE in the application of analysis of tap water sample.

2. Experimental

2.1. Materials

MWCNTs were obtained from Chengdu Institute of Organic Chemistry (China). Hydroquinone (HQ) and catechol (CC) were provided from Sigma-Aldrich (USA). $MnSO_4 \cdot H_2O$, $(NH_4)_2S_2O_8$ and other reagents were purchased from Sinopharm Co. (China) with analytical grade purity. For study of pH effect 0.1 M phosphate buffer solutions (PBS) of pH 5.0–8.0 were used. The stock solution (1×10^{-3} M) of HQ or CC was freshly prepared by dissolving HQ or CC in a PBS (0.1 M, pH 7.0). The water used was double-distilled.

2.2. Preparation of the hydroquinone and catechol sensor

MWCNTs were treated with concentrated HNO_3 during purification process followed by filtering, rinsing with double-distilled water and drying in air. The preparation of nanosized MnO_2 was adapted from the previous report [26]. In a typical synthesis, 0.008 mol of $MnSO_4 \cdot H_2O$ and an equal amount of $(NH_4)_2S_2O_8$ were put into distilled water to form a homogeneous solution, which was then transferred into an autoclave, sealed, and heated at 120 ℃ for 12 h. The autoclave was then naturally allowed to cool to room temperature. The resulting black solid product was filtered, washed with water to possibly remove remnant ions in the final products, and dried at 120 ℃ in oven. Then, MWCNTs was mixed with nanosized MnO_2 on a weight ratio of 1.5:1 in an agate mortar and ground for 2 h by hand, producing a black-brown colloidal powder with uniform color, a suspension of 2 mg·mL^{-1} was prepared by dispersing

4 mg of colloidal powder in 2 mL 1:1 DMF (v/v) by ultrasonication for 30 min. The final solution was denoted as MWCNTs-MnO_2.

The glassy carbon electrode (GCE) was polished with 1, 0.3 and 0.05 μm alumina powder, respectively, and then washed ultrasonically in 1:1 HNO_3 (v/v), ethanol and doubly distilled water for 30 s, respectively. 7 μL of the MWCNTs-MnO_2 suspension (2 $mg\cdot mL^{-1}$) was coated onto the surface of GCE and drying in air. A MWCNTs-MnO_2 modified GCE was obtained. The MWCNTs/GCE and MnO_2/GCE were prepared through similar procedure for comparison.

2.3. Apparatus

The electrochemical experiments were done using a CHI660C electrochemical workstation (ShangHai ChenHua Instruments, China). A conventional three-electrode system was used in the experiments, with GCE (Φ = 3 mm), MWCNTs/GCE, MnO_2/GCE or MWCNTs-MnO_2/GCE as the working electrode, an Ag/AgCl as the reference electrode and a platinum wire as the counter electrode, respectively. All potentials in this paper were referred to Ag/AgCl electrode. Cyclic voltammetric experiments were performed in the potential range −0.5 V to +0.2 V with a scan rate of 50 $mV\cdot s^{-1}$. The electrochemical parameters for differential pulse voltammetry (DPV) were as follows: pulse amplitude: 50 mV, pulse width: 50 ms, pulse increment: 4 mV.

Electrochemical impedance spectroscopy (EIS) was carried out using Princeton PARSTAT4000 between 0.1 Hz and 10 kHz at 0.25 V. Scanning electron microscopy (SEM) images were obtained with a Carl Zeiss EVO18 (German) operating at 20 kV. Energy-dispersive X-ray spectroscopy (EDX) was recorded using a BRUKER quantax 200 (German). Ultrasonic cleaner (BRANSON2000, USA) was used in this experiment. The pH value of PBS was measured with a pHS-3C meter (Leici Devices Factory of Shanghai, China).

3. Results and Discussion

3.1. Characterizations of modified electrode

The surface morphologies of different films were characterized by SEM. As expected, a MWCNTs layer showed a wrinkled structure (Fig. 1(a)). As shown in Fig. 1(b), a claviform-like structure of MnO_2 nanowires with diameters 40-60 nm was observed. In contrast, a well distribution of MnO_2 nanowires in MWCNTs matrix was displayed in Fig. 1(c) when MnO_2 and MWCNTs were mixed together. The EDX spectrum of MWCNTs-MnO_2 composite film was depicted in Fig. 1(d), the elements C, Mn and O were detected in the composite film.

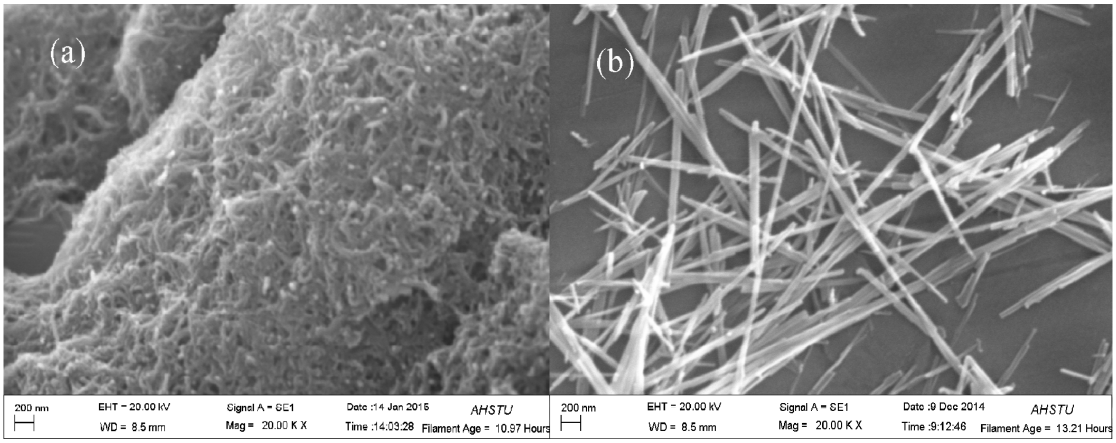

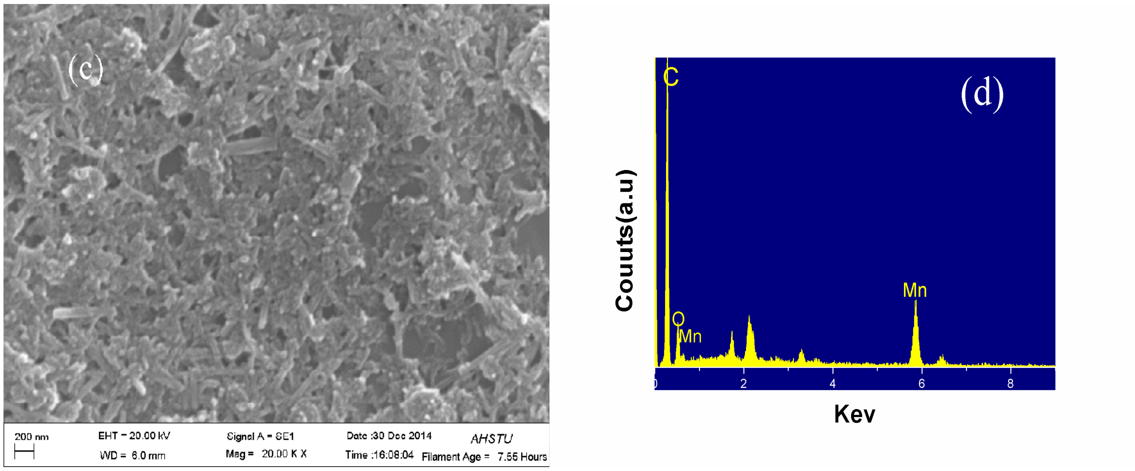

Fig. 1. SEM image of MWCNTs film (a), MnO_2 nanowires (b), MWCNTs-MnO_2 composite film (c) and EDX spectrum of MWCNTs-MnO_2 composite film (d)

EIS is an effective tool for probing the interfacial charge-transfer kinetics on the surface of modified electrodes [27]. EIS measurements were carried out by using $[Fe(CN)_6]^{3-/4-}$ (1 : 1; 5 $\times 10^{-3}$ M) as the redox mediator to study the surface property of different electrodes. The Randles equivalence circuit (Fig. 2 inset) included the electrolyte resistance (R_s), Warburg impedance (Z_w), charge transfer resistance (R_{ct}) and double layer capacitance (C_{dl}). The curve of EIS included a linear portion and a semicircle portion. The semicircle portion at higher frequencies represented the electron transfer limited process and the diameter of the semicircle was equivalent to the charge transfer resistance (R_{ct}). As shown in Fig. 2 (curve a), a big semicircle portion indicated a poor interfacial charge transfer at MnO_2/GCE. However, the curve of the bare GCE (curve b), MWCNTs/GCE (curve c) and MWCNTs-MnO_2/GCE (curve d) exhibited smaller diameter of the semicircles compared with the MnO_2/GCE. MWCNTs-MnO_2/ GCE showed the smaller R_{ct} value than others, suggesting that poor charge transfer of MnO_2/GCE could be overcome by the incorporation of the MWCNTs. The results indicated that fast charge transfer took place at the MWCNTs-MnO_2/GCE facilitated by highly conducting materials in the composite film.

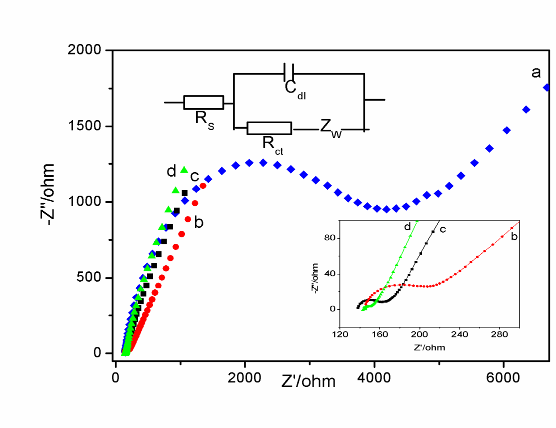

Fig. 2. Nyquist plots of (a) MnO_2/GCE , (b) bare GCE, (c) MWCNTs/GCE and (d) MWCNTs-MnO_2/GCE in 5 $\times 10^{-3}$ M $[Fe(CN)_6]^{3-/4-}$ containing 0.1 M KCl . Inset: the equivalent circuit and the enlargement of the plots of (b) bare GCE, (c) MWCNTs/GCE and (d) MWCNTs-MnO_2/GCE.

3.2 Electrooxidation behavior of HQ and CC

The cyclic voltammetric responses for the different electrodes in the 0.1M PBS solution (pH 7.0) containing

1×10^{-4} M HQ and 1×10^{-4} M CC were shown in Fig. 3. When the bare GCE was chosen as the working electrode (curve a), two small reduction peaks appeared and accompanied with one broad oxidation peak, indicating the overlapping of electrochemical responses of HQ and CC. So the redox responses of HQ and CC could not be distinguished in this instance. Interestingly, this situation changed when the modified GCEs were used to replace the bare GCE. While at MnO_2/GCE (curve c) two pairs of redox peaks appeared. The result could be attributed to excellent electrocatalytic properties of MnO_2. MWCNTs/GCE (curve b) exhibited well defined redox peaks of HQ and CC appeared with increased peak current, implying the modification of MWCNTs effectively increased the surface area of the electrode. At MWCNTs-MnO_2/ GCE (curve d) the redox peaks of HQ and CC were well separated, well defined and with higher currents than at MWCNTs/GCE (curve b) and MnO_2/GCE (curve c). Additionally, it can be seen from Fig. 3 (curve e) that there was a large background current at MWCNTs-MnO_2/GCE, which was caused by a larger surface area of the composite film at GCE. HQ showed redox peaks at −121 mV and −153 mV with $\triangle E$ of 32 mV. CC showed redox peaks at −19 mV and −49 mV with $\triangle E$ of 30 mV. Because of the separation between peak potentials were very small and the ratio of the anodic peak currents to the cathodic peak currents was equal to unity, the redox reactions of HQ and CC can be used as ideal Nernst equation, the number of electrons of both HQ and CC were given by [28]: $\triangle E_{p,1/2} = 3.53RT/nF = 90.6/n$, calculated as $n = 2$, which is in good agreement with previous report [29]. Also the separation of the oxidation peak potential of HQ and CC was calculated as 102 mV, bigger enough for the quantitative and qualitative determination of HQ and CC.

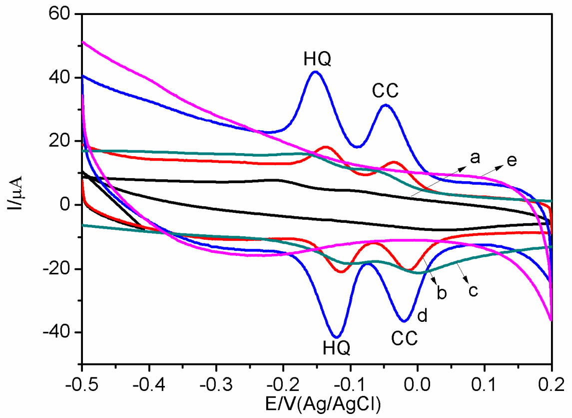

Fig. 3. CVs of a mixture solution of 1×10^{-4} M HQ and 1×10^{-4} M CC at (a) bare GCE, (b) MWCNTs/GCE, (c) MnO_2/GCE and (d) MWCNTs-MnO_2/GCE. Curve e corresponding to blank PBS solution (pH 7.0) at MWCNTs-MnO_2/GCE. Scan rate: 50 $mV\cdot s^{-1}$

The improved electrochemical behavior of MWCNTs-MnO_2 mainly attributed to their high surface area and excellent catalytic activity. Based on obtained results which indicated a $2e^{-}$ mechanism for HQ and CC, MnO_2 acted as an electron transfer mediator [30] to accelerate electron transfer rate for oxidation of HQ and CC, the mediator being regenerated. The schematic diagram of the detection principle was shown in Scheme. 1. Therefore, HQ and CC were effectively detected at the MWCNTs-MnO_2 modified GCE.

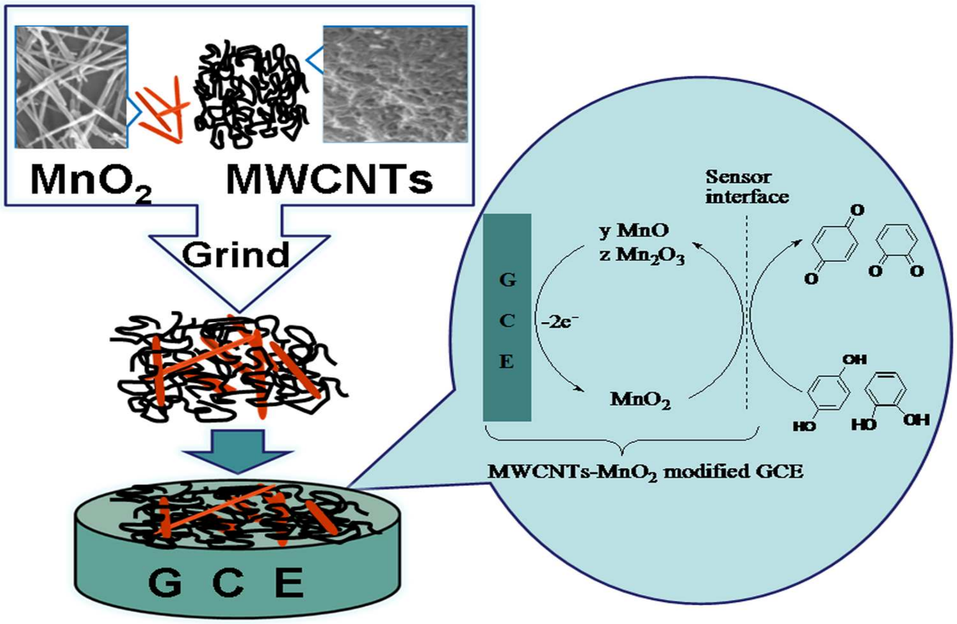

Scheme 1 Proposed reaction mechanism of HQ and CC at MWCNTs-MnO_2 modified GCE

3.3. Selection of the experimental conditions

3.3.1 Effect of solution pH

Acidity of electrolyte has a significant effect on the HQ and CC electrooxidation because protons participate in the electrode reaction. In this work, some supporting electrolytes, such as phosphate buffer solution (NaH_2PO_4-Na_2HPO_4, PBS), NaOH-KH_2PO_4, acetate buffer solution (HAc-NaAc) and Britton-Robinson buffer solution (B-R) were investigated to optimize the response of HQ and CC at MWCNTs-MnO_2/GCE. Experimental results showed that in NaH_2PO_4-Na_2HPO_4 buffer solution, both HQ and CC exhibited well-defined and sensitive peaks. Thus, aqueous PBS was chosen as the supporting electrolyte. The effect of pH value of HQ and CC at MWCNTs-MnO_2/GCE was investigated in PBS over a pH range of 5.0-8.0 (Fig. 4(A) and 4(B)). The anodic peak potentials of both HQ and CC shifted negatively with increasing pH from 5.0 to 8.0 (Fig. 4(C)), indicating a direct participation of protons in the oxidation process [31]. Both E_{pa} values of HQ and CC were proportional to the pH value and the regression equations can be expressed as: E_{pa} (HQ) = 0.327−0.0642 pH (R=0.9915) and E_{pa} (CC) = 0.362−0.0566 pH (R=0.9901), respectively. These two almost parallel lines (Fig. 4(C)) indicated that the peak potential difference between HQ and CC was constant. The slopes of these equations were close to the expected value of −59 mV/pH as obtained from the Nernst equation (298 K), suggesting equal numbers of proton-transfer and electron-transfer [32] for electrochemical oxidation of HQ and CC at MWCNTs-MnO_2/GCE. In summary, both of HQ and CC took place a two-electron, two-proton nearly reversible reaction at MWCNTs-MnO_2/GCE.

Fig. 4(D) revealed that oxidation peak currents of two isomers reached the maximum value at pH 7.0, then decreased with further increase of pH. Overall, pH 7.0 was chosen as the optimal experimental condition in the following experiments.

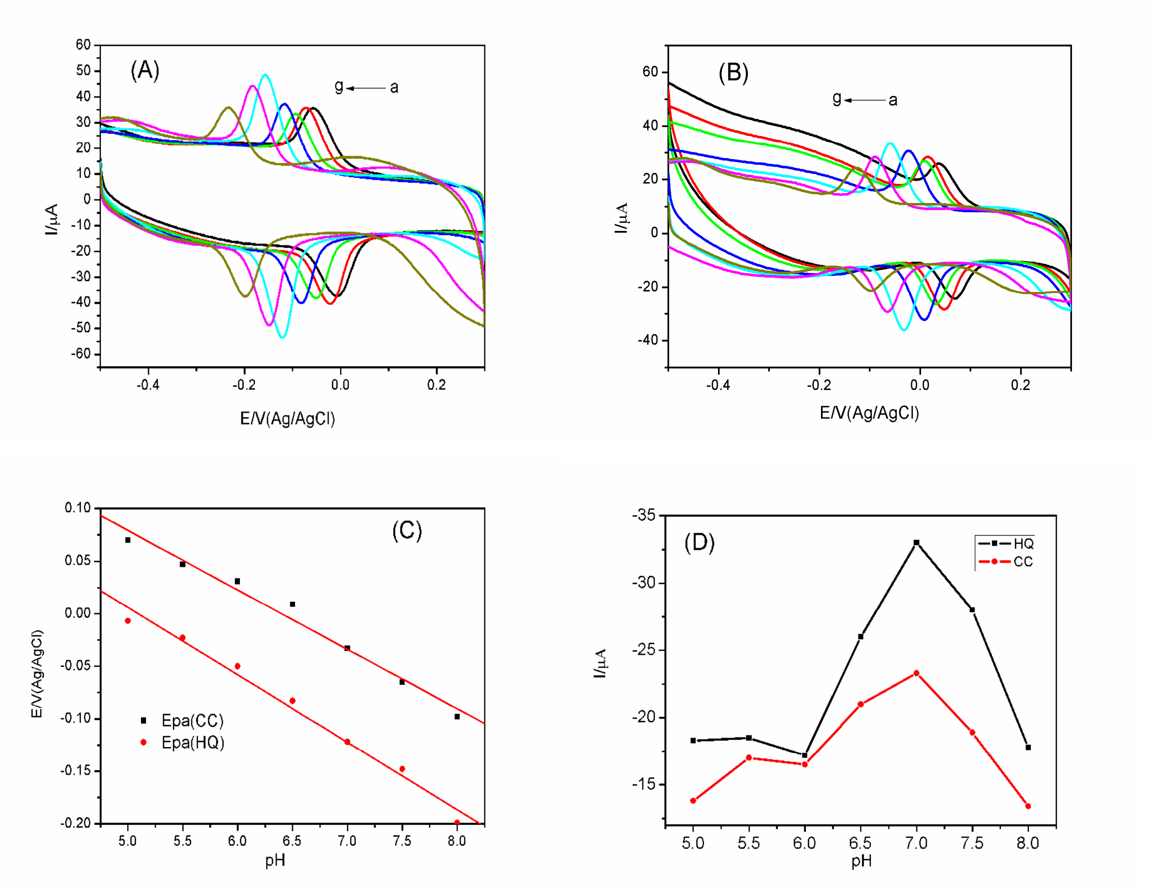

Fig. 4. CVs of MWCNTs-MnO_2/GCE in pH 5.0–8.0 PBS containing 1×10^{-4} M HQ (A) and 1×10^{-4} M CC (B) (pH value from a to g: 5.0, 5.5, 6.0, 6.5, 7.0, 7.5, 8.0). (C) E_{pa}–pH relationship of HQ and CC. (D) I_{pa}–pH relationship of HQ and CC.

3.3.2. Effect of scan rate

The influence of scan rate on the electrochemical behavior of a mixture of 1×10^{-4} M HQ and 1×10^{-4} M CC in 0.1 M PBS (pH 7.0) was further examined at MWCNTs-MnO_2/GCE by CV. Both the anodic and cathodic peak currents of HQ and CC enhanced with increasing the scan rate from 10 to 100 $mV\cdot s^{-1}$. As shown in Fig. 5(B), a good linear relationship between the peak current (I) and the scan rate (v) was obtained. The corresponding linear regression equations were: HQ: I_{pc} (μA) = $0.5050v + 2.9013$ (v in $mV\cdot s^{-1}$) (R=0.9972) and I_{pa} (μA) = $-0.6123v - 3.2053$ (R=0.9972), CC: I_{pc} (μA) = $0.4507v + 3.1773$ (v in $mV\cdot s^{-1}$) (R=0.9972) and I_{pa} (μA) = $-0.5287v - 2.3133$ (v in $mV\cdot s^{-1}$) (R=0.9974). This linearity demonstrated that the redox reaction of HQ and CC was a typical adsorption-controlled process.

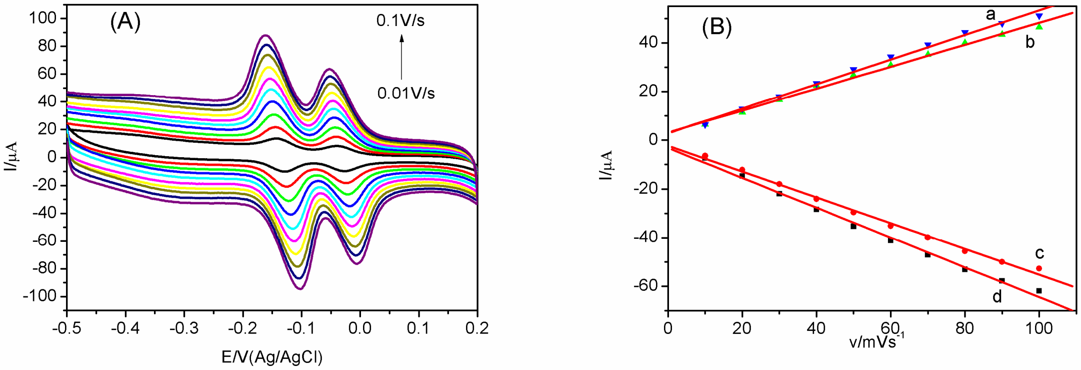

Fig. 5. (A) CVs of MWCNTs-MnO_2/GCE with 1×10^{-4} M HQ and CC in PBS (pH 7.0) at different scan rates from inter to outer: 10, 20, 30, 40, 50, 60, 70, 80, 90, 100 mV·s^{-1}. (B) The dependence relationship between redox peak current and scan rate for HQ (curve a and d) and CC (curve b and c).

3.4. Simultaneous determination of HQ and CC using differential pulse voltammetry

Differential pulse voltammetry (DPV) was employed for the simultaneous determination of HQ and CC at MWCNTs-MnO_2/GCE because of its higher current sensitivity and better resolution compared with CV. The individual determination of HQ or CC in their mixtures was first performed at the MWCNTs-MnO_2/GCE when the concentration of one species was a constant. Examination of Fig. 6(A) showed that the oxidation peak current of HQ increased with an increase in the HQ concentration while the concentration of CC was kept constant (5×10^{-5} M). From the inset of Fig. 6(A), the oxidation peak current of HQ was linear with its concentration in the range of 5×10^{-7} M – 8×10^{-5} M. The regression equation was I_{pa} (μA) =−1.1320C (μM)−9.5998 (R=0.9968), the detection limit for HQ was estimated to be 5×10^{-8} M (S/N = 3). Similarly as shown in Fig. 6(B), kept the concentration of HQ constant as 5×10^{-5} M, the oxidation peak current was proportional to the concentration of CC from 5×10^{-7} M to 8×10^{-5} M, and the LOD was 8×10^{-8} M (S/N = 3). The regression equation was I_{pa} (μA) =−1.2083C (μM)−2.3739 (R=0.9963). It can be seen that the presence of isomer did not interfere with the electrochemical detection of another compound, which indicated that MWCNTs-MnO_2/GCE exhibited good distinguish ability for individual HQ or CC detection.

Fig. 6(C) showed DPV curves of HQ and CC in the mixture solution by simultaneously changing their concentrations. Two well-defined oxidation peaks appeared and the separation of the oxidation peak potentials of HQ and CC was got as 102 mV. The oxidation peak currents (I_{pa}) of HQ and CC increased linearly with their concentrations from 5×10^{-7} M to 8×10^{-5} M. The regression equations were I_{pa} (μA) =−1.1340C (μM)−9.4509 (R=0.9958) for HQ and I_{pa} (μA) =−0.9323C (μM)−8.9954 (R=0.9972) for CC, respectively. To the best of our knowledge, this is the first time that MWCNTs-MnO_2/ GCE can be used effectively for simultaneous determination of HQ and CC without interference with each other. A comparison of the proposed method with other modified electrodes for simultaneous detection HQ and CC was summarized in Table 1. It showed that the linear range of HQ and CC at the present work was wider, and the detection limit was lower than that most published works. Therefore, MWCNTs-MnO_2 composite modified electrode was a competitive candidate in simultaneous determination of dihydroxybenzene isomers compared with other modified electrodes.

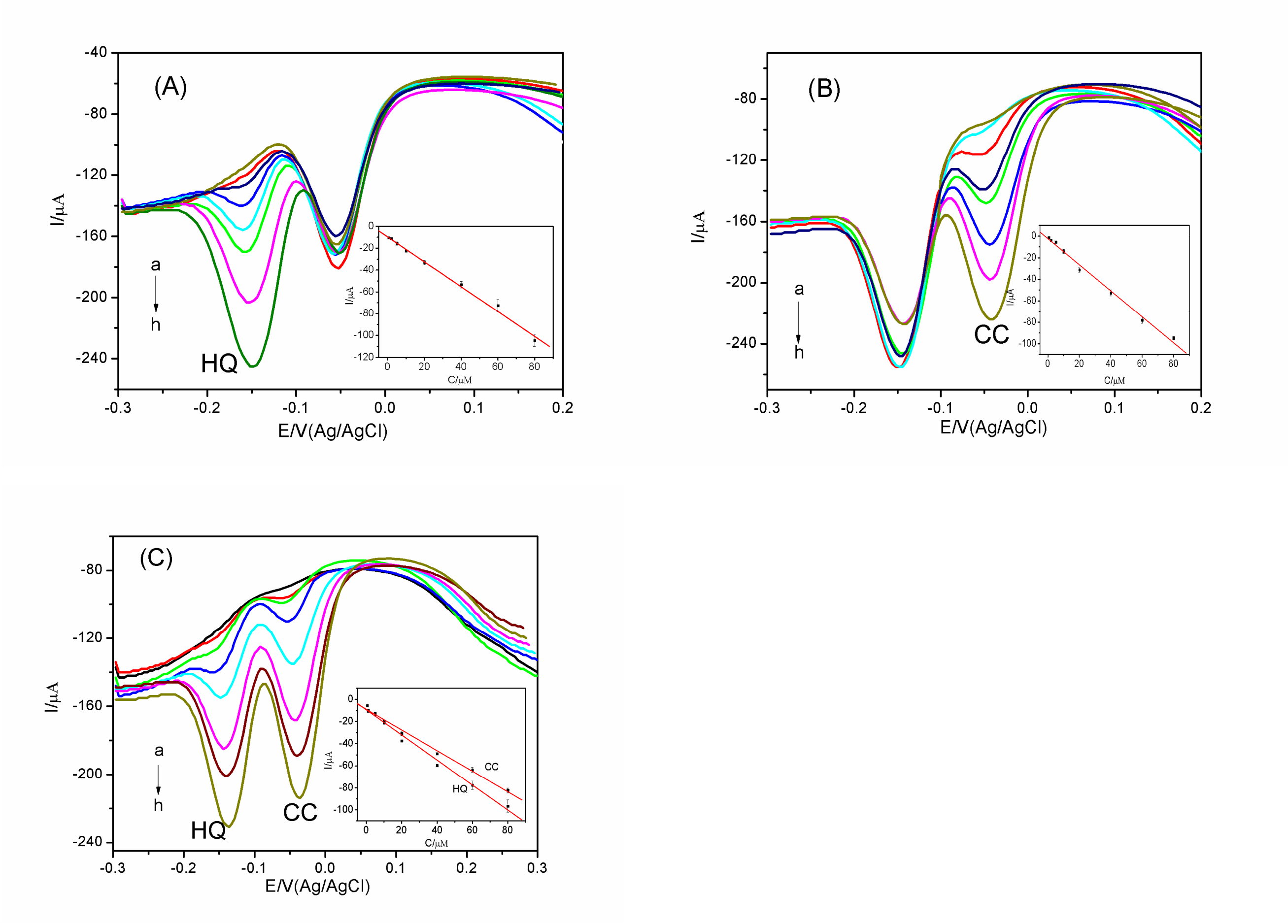

Fig. 6. (A) DPV of HQ at MWCNTs-MnO$_2$/GCE in the presence of 5×10^{-5} M CC and HQ concentrations (from a to h): (a) 5×10^{-7} M, (b) 2×10^{-6} M, (c) 5×10^{-6} M, (d) 1×10^{-5} M, (e) 2×10^{-5} M, (f) 4×10^{-5} M, (g) 6×10^{-5} M, (h) 8×10^{-5} M. Inset the dependence of the HQ peak currents on concentrations. Supporting electrolyte: 0.1 M PBS (pH 7.0) (B) DPV of CC at MWCNTs-MnO$_2$/GCE in the presence of 5×10^{-5} M HQ and CC concentrations (from a to h): (a) 5×10^{-7} M, (b) 2×10^{-6} M, (c) 5×10^{-6} M, (d) 1×10^{-5} M, (e) 2×10^{-5} M, (f) 4×10^{-5} M, (g) 6×10^{-5} M, (h) 8×10^{-5} M. Inset the dependence of the CC peak currents on concentrations. (C) DPV of various concentrations of HQ and CC (from (a) to (h): (a) 5×10^{-7} M, (b) 1×10^{-6} M, (c) 5×10^{-6} M, (d) 1×10^{-5} M, (e) 2×10^{-5} M, (f) 4×10^{-5} M, (g) 6×10^{-5} M, (h) 8×10^{-5} M, Inset the relationship of the oxidation peak current with the concentration of HQ and CC.

Table 1 Comparison of analytical performances at different materials-based electrochemical sensors for the simultaneous electrochemical determination of HQ and CC.

Modified electrodes	Analytes	Supporting electrolyte	Linear range (μM)	Detection limit (nM)	Reference
Ordered mesoporous carbon/GCE	HQ	0.1 M pH 5.0 K_2HPO_4–KH_2PO_4	10-200	76	[12]
	CC		10-300	100	
GO–MnO$_2$/GCE[a]	HQ	pH 7.0 Na_2HPO_4-$C_4H_2O_7$	0.03-1	0.13	[33]
	CC		0.01-0.7	0.1	
RGO–MWCNTs/GCE[b]	HQ	0.1 M pH 7.0 PBS	8.0-391	2600	[34]
	CC		5.5-540	1800	
GR-La(OH)$_3$/GCE[c]	HQ	0.1 M pH 4.0 Na_2HPO_4-$C_4H_2O_7$	5-300	15	[35]
	CC		5-300	10	
CNTs/ionic liquid /GCE	HQ	0.1 M pH 7.0 PBS	0.2-35	180	[36]
	CC		0.18-35	60	

PIL–MWCNTs/GCE[d]	HQ	0.1 M pH 7.0 PBS	1-500	400	[37]
	CC		1-400	170	
Carbon nanoparticle -chitosan composite	HQ	0.1 M pH 7.0 PBS	0.8-100	200	[38]
	CC		0.8-100	200	
MWCNTs/GCE	HQ	0.10 M pH 5.0 HAc-NaAc	2-100	600	[9]
	CC		2-100	600	
Pt/ZrO_2−RGO/GCE	HQ	0.05M pH 7.0 PBS	1-400	400	[39]
	CC		1-1000	400	
GR–TiO_2/GCE	HQ	0.1 M pH 7.0 PBS	0.5-100	87	[40]
	CC		0.5-100	82	
TiO_2/MWCNTs/GCE	HQ	0.1 M pH 7.0 PBS	1.5-300	800	[41]
	CC		2.5-200	800	
Pt–MnO_2/GCE	HQ	0.1 M pH 7.0 PBS	3-481	-	[23]
	CC		15-447	-	
MWCNTs-MnO_2/GCE	HQ	0.1 M pH 7.0 PBS	0.5-80	50	This work
	CC		0.5-80	80	

[a] GO: graphene oxide. [b] RGO-MWCNTs: reduced graphene oxide- multi-walled carbon nanotubes. [c] GR: graphene.

[d] PIL: polymeric ionic liquid

3.5. Repeatability, reproducibility, stability and selectivity of MWCNTs-MnO_2/GCE

The repeatability of MWCNTs-MnO_2/GCE was investigated by measuring the response to the mixed solution containing 5×10^{-5} M HQ and 5×10^{-5} M CC. The relative standard deviation (*RSD*) for HQ and CC in five successive measurements was 2.22 % and 3.12%, respectively, indicating an excellent repeatability of MWCNTs-MnO_2 /GCE. The fabrication reproducibility was estimated by using four modified electrodes independently prepared by the same procedure, the RSD was 3.52% and 3.87% for HQ and CC, respectively. Additionally, the stability of MWCNTs-MnO_2/GCE was explored. Even if the modified electrode was stored at 4 °C for 2 weeks, the current responses still retained more than 92 % of the initial response. This suggested that the MWCNTs-MnO_2/GCE has good repeatability and reproducibility along with a considerable average stability.

The interference from some common ions and other organic compounds were examined with 5.0×10^{-5} M HQ and CC in 0.1 M PBS (pH 7.0). Experimental results showed that 1000-fold K^+, Na^+, Ca^{2+}, Pb^{2+}, Ni^{2+}, Zr^{2+}, Fe^{3+}, Cu^{2+}, Mg^{2+}, NO_3^-, SO_4^{2-}, $CO_3^{2-}$and 100-fold Fe^{3+}, S^{2-}, ascorbic acid, uric acid do not interfere with the determination (signal change below 5%). Moreover, 5-fold phenol, resorcinol and nitrophenol had no effect on the determination, implying a high selectivity and favorable ability of anti-interference at MWCNTs-MnO_2/GCE.

3.6. Analytical application

To evaluate the practical feasibility of the proposed method, the MWCNTs-MnO_2/GCE was applied for the simultaneous determination of HQ and CC in local tap water (Hefei, PR China). The recovery experiments were performed by measuring the DPV responses to the samples in which the known concentrations of HQ and CC were added. The amounts of HQ and CC in the tap water samples were determined by calibration method and the results were listed in Table 2. The recoveries were 98.57–103.20% for HQ and 98.72–101.15% for CC, respectively. A practical applicability and good reliability of the fabricated electrode for direct simultaneous determination of HQ and CC were evident.

Table 2 Simultaneous determination of HQ and CC in tap water samples

Sample	Analyte	Added (μM)	Found[a] (μM)	RSD[b] (%)	Recovery (%)
1	HQ	10	9.89±0.15	1.69	98.90
	CC	60	60.69±0.18	1.93	101.15
2	HQ	20	20.64±0.22	2.33	103.20
	CC	50	49.92±0.13	2.18	99.84
3	HQ	30	29.57±0.19	1.45	98.57
	CC	40	39.49±0.16	1.76	98.72
4	HQ	40	40.28±0.25	2.12	100.70
	CC	30	29.77±0.21	1.96	99.23

[a] Standard addition method. [b] Relative standard deviation for 5 successive measurements.

4. Conclusions

A MWCNTs-MnO_2 nanocomposite modified electrode was fabricated by a simple grinding method and applied for simultaneous determination of HQ and CC. The EIS studies revealed high charge transfer resistance at MnO_2 modified electrode and could be reduced by the incorporation of MWCNTs film. The MWCNTs-MnO_2 composite modified electrode exhibited two couples of independent well-defined redox peaks and increase of peak currents toward HQ and CC, which could be attributed to their excellent catalytic activity, high surface area and nanosized structure. Electrochemical behaviors of HQ and CC at MWCNTs-MnO_2/GCE were absorption-controlled nearly reversible processes with two electrons and two protons involved in the electrode reaction. In addition, the MWCNTs-MnO_2 modified electrode showed low detection limit, wide linear range, good reproducibility and long-term stability. This method was applied to the direct determination of HQ and CC in tap water with satisfactory recovery results. Moreover, MWCNTs and MnO_2 composite had good synergistic effects with great potential for further application.

Acknowledgements

This work was supported by the National Nature Foundation of China (Grants No. 21175001), Doctoral Program Foundation of the Ministry of Education of China (20103401110001), the Foundation of Scientific Innovation Team of Anhui Province (2006KJ007TD), Foundation of Anhui Science and Technology University (ZRC2014438) and the 211 Project of Anhui University.

References

[1] J. Wang, J. N. Park, X. Y. Wei and C. W. Lee, *Chem. Commun.,* 2003, 5, 628.
[2] H. Zhang, J. S. Zhao, H. T. Liu, R. M. Liu, H. S. Wang and J. F. Liu, *Microchim. Acta,* 2010, 169, 277.
[3] I. Buttino, M. Flippi and N. Cardellicchio, *Acqua. Aria*, 1991, 9, 853.
[4] H. Cui, C. X. He and G. W. Zhao, *J. Chromatogr. A,* 1999, 855, 171.
[5] A. Asan and I. Isildak, *J. Chromatogr. A*, 2003, 988, 145.
[6] S. F. Li, X. Z. Li, J. Xu and X. W. Wei, *Talanta*, 2008, 75, 32.
[7] A. Afkhami and H. A. Khatami, *J. Anal. Chem.*, 2001, 56, 429.
[8] W. Sun, Y. H. Wang, Y. X. Lu, A. H. Hu, F. Shi and Z. F. Sun. *Sens. Actuators, B*, 2013, 188, 564.
[9] H. L. Qi and C. X. Zhang, *Electroanalysis*, 2005, 17, 832.

[10] J. Du, L. L. Ma, D. L. Shan, Y. R. Fan, L. P. Zhang, L. Wang and X. Q. Lu, *J. Electroanal. Chem.*, 2014, 722-723, 38.

[11] M. A. Ghanem, *Electrochem. Commun.,* 2007, 9, 2501.

[12] J. Bai, L. P. Guo, J. C. Ndamanisha and B. Qi, *J. Appl. Electrochem.,* 2009, 39, 2497.

[13] D. Salinas-Torresa, F. Huertab, F. Montillaa and E. Morallóna, *Electrochim. Acta*, 2011, 56, 2464.

[14] S. K. Kim, D. Kim, J. M. You, H. S. Han and S. Jeon, *Electrochim. Acta*, 2012, 81, 31.

[15] Y. L. Cao, R. Yuan, Y. Q. Chai, L. Mao, H. Niu, H. J. Liu and Y. Zhuo, *Biosens. Bioelectron.*, 2012, 31,305.

[16] M. Devaraj, R. K. Deivasigamani and S. Jeyadevan, *Colloids Surf. B,* 2013,102, 554.

[17] M.F. Wang, C. Wang, G.F. Wang, W. Zhang and F. Bin, *Electroanal.*, 2010, 22,1123.

[18] J. Zolgharnein, T. Shariatmanesh and A. Babaei, *Sens. Actuators, B,* 2013, 186, 536.

[19] S. J. Bao, B. L. He, Y. Y. Liang, W. J. Zhou and H. L. Li, *Mater. Sci. Eng., A*, 2005, 397, 305.

[20] S. J. Yao, S. Yuan, J. H. Xu, Y. Wang, J. L. Luo and S. S. Hu, *Appl. Clay Sci.,* 2006, 33, 35.

[21] Y. J. Yang and S. Hu, *Electrochim. Acta,* 2010, 55, 3471.

[22] D. Das, P. R. Samaddar, P. K. Sen and K. Das, *J. Appl. Electrochem.*, 2008, 38, 743.

[23] B. Unnikrishnan, P. L. Ru and S. M. Chen, *Sens. Actuators, B*, 2012, 169, 235.

[24] L. Q. Luo, F. Li, L. M. Zhu, Z. Zhang, Y. P. Ding and D. M. Deng, *Electrochim. Acta*, 2012, 77, 179.

[25] J. Chen, W.D. Zhang and J. S. Ye, *Electrochem. Commun.*, 2008, 10, 1268.

[26] X. Wang and Y. D. Li, *J. Am. Chem. Soc.,* 2002, 124, 2880.

[27] F. Patolsky, M. Zayats, E. Katz and I. Willner, *Anal. Chem.*, 1999, 71, 3171.

[28] A. J. Bard and L. R. Faulkner, Electrochemical methods: fundamentals and applications, second ed, Viley, New York, 2001 (Chaps. 14 pp 591).

[29] H. J. Du, J. S. Ye, J. Q. Zhang, X. D. Huang and C. Z. Yu, *J. Electroanal. Chem.,* 2011, 650, 209.

[30] N. W. Beyene, P.Kotzian, K. Schachl, H. Alemu, E. Turkušić, Amira Čopra, H. Moderegger, I.Švancara, K. Vytřas and K. Kalcher. *Talanta*, 2004, 64, 1151.

[31] D. Nematollahi, H. Shayani-Jam, M. Alimoradi and S. Niroomand, *Electrochim. Acta,* 2009, 54, 7407.

[32] L. T. Wang, Y. Zhang, Y. L. Du, D. B. Lu, Y. Z. Zhang and C. M. Wang, *J. Solid State Electrochem.,* 2012, 16, 1323.

[33] T. Gan, J. Y. Sun, K. J. Huang, L. Song and Y. M. Li, *Sens. Actuators, B,* 2013, 177, 412.

[34] F. X. Hu, S. H. Chen, C. Y. Wang, R. Yuan, D. H. Yuan and C. Wang, *Anal. Chim. Acta,* 2012, 724, 40.

[35] Z. Guo, Y. Lu, J. Li, X.F. Xu, G.Q. Huang and Z.Y. Wang. *Anal. Methods,* 2014, 6, 8314.

[36] C. H. Bu, X. H. Liu, Y. J. Zhang, L. Li, X. B. Zhou and X. Q. Lu, *Colloids Surf. B,* 2011, 88, 292.

[37] X. Feng, W. W. Gao, S. H. Zhou, H. Y. Shi, H. Huang and W. B. Song, *Anal. Chim. Acta,* 2013, 805, 36.

[38] M. Amiri, S. Ghaffari, A. Bezaatpour and F. Marken, *Sens. Actuators, B,* 2012, 162, 194.

[39] A. T. E. Viliana, S. M. Chen, L. H. Huang, M. A. Alib and F. M. A. AlHemaid. *Electrochim. Acta,* 2014, 125, 503.

[40] Y. L. Zhang, S. X. Xiao, J. L. Xie, Z. M. Yang, P. F. Pang and Y. T. Gao, *Sens. Actuators, B,* 2014, 204, 102.

[41] Z. C. Meng, H. F. Zhang and J. B. Zheng, *Res. Chem. Intermed,* 2013, 39, DOI: 10.1007/s11164-013-1420-9.

A graphical and textual abstract for the contents pages

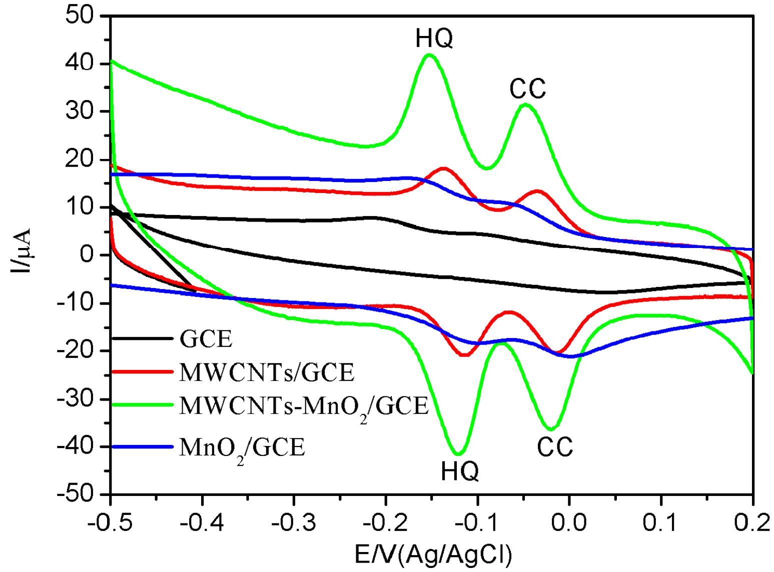

Cyclic voltammograms of a mixture solution of 0.1 mM HQ and 0.1 mM CC at bare GCE, MWCNTs/GCE, MnO_2/GCE and MWCNTs-MnO_2/GCE.